南京航空航天大学

论文集

（二〇〇八年） 第27册

机电学院

（第4分册）

南京航空航天大学科技部编

二〇〇九年五月

机电学院

054系

序号	姓名	职称或学历	单位	论文题目	刊物、会议名称	年、卷、期
1	范国强 高霖	博士生 教授	054	Electric hot incremental forming: A novel technique	International Journal of Machine Tools & Manufacture	2008年48卷
2	古·侯赛因纳·哈亚特 高霖	博士生 教授 教授	054	An experimental study on effect of thinning band on sheet formability in negative incremental forming	International Journal of Machine Tools & Manufacture	2008年 48 卷
3	古·侯赛因 高霖	博士生 教授	054	Formability evaluation of a pure titanium sheet in the cold incremental forming process	International Journal of Advanced Manufacturing Technology	2008年37卷
4	古·侯赛因 高霖	博士生 教授	054	Tool and lubrication for negative incremental forming of a commercially pure titanium sheet	Journal of materials processing technology	2008年 203卷
5	王辉 郑毅 高霖	博士生 高工 教授	054	差厚激光拼焊板的成形极限	机械工程材料	2008年32卷4期
6	崔震 高霖 陆启建	博士生 教授 高工	054	数控渐进成型技术在圆孔翻边中的应用	机械工程材料	2008年 32 卷
7	崔震 高霖 徐岩	博士生 教授 副教授	054	数控渐进成形中的鼓包问题分析	机械科学与技术	2008年27卷12期
8	彭文 高霖	硕士生 教授	054	基于虚拟仪器技术的涡轮增压器试验台研究	国外电子测量技术	2008年11期
9	方挺立 黄　翔 李迎光	博士生 教　授 教　授	054	飞机结构件加工特征定义方法研究	机械科学与技术	2008, 27(8)
10	潘志毅 黄　翔 李迎光	博士生 教　授 教　授	054	有向图向设计结构矩阵与多色集合同步映射的设计过程规划方法	计算机集成制造系统	2008, 14(7)
11	潘志毅 黄　翔 李迎光	博士生 教　授 教　授	054	飞机制造大型工装布局设计方法研究与实现	航空学报	2008, 29(3)
12	刘海燕 金　霞	硕士 讲师	054	板料成形的回弹预测方法研究	机械制造与自动化	2008, 37（6）
13	金　霞 鲁世红 孙家军 于长生	讲师 副教授 硕士 硕士	054	单轴柔性滚弯成形的有限元分析	机械科学与技术	2008, 27(12)
14	闫崇京 廖和文 郭宇 程悠胜	讲师 教授 副教授 教授	054	基于多色图的BOM建模	山东大学学报（工学版）	2008, 38(6)
15	鲁世红 谢卿阳	副教授 研究生	054 054	Study on Adiabatic Shear Behavior in Orthogonal Cutting for H13 Steel	Advanced Design and Manufacture to Gain a Competitive Edge	2008
16	鲁世红 金　霞 步　娟	副教授 讲师 研究生	054 054 054	Experimental Research and FEM analysis of the Two-Axle Rotary Shaping with Elastic Medium	Advanced Design and Manufacture to Gain a Competitive Edge	2008

17	鲁世红 何宁	副教授 教授	054	高应变速率下Al-Mg-Sc合金压缩变形的流变方程.	中国有色金属学报,	2008, 18(5): 897-902 .
18	鲁世红 何宁	副教授 教授	054	H13淬硬钢高应变速率动态性能的实验与本构方程研究.	中国机械工程,	2008, 19(19): 2382-2385.
19	卫炜 周来水 王志国	副教授 教　授 讲　师	054	NURBS曲面上的曲线精确表达	南京航空航天大学学报	2008, 40(1)
20	谭昌柏 周来水 张丽艳 卫炜 王志国 汪俊	讲师 教授 教授 副教授 讲师 博士生	054	飞机外形和结构件反求建模技术研究	航空学报	2008, 29(6)
21	孟辉 安鲁陵	硕士生 教　授	054	基于DSP外部扩展总线接口的键盘实现方法	仪器仪表用户	2008，15（1）
22	马玉伟 安鲁陵	硕士生 教　授	054	均匀偏置型腔加工残留区域分析	机械制造与自动化	2008，37（2）
23	张富官 安鲁陵 李汝鹏	硕士生 教　授 硕士生	054	复合材料构件成型模具的参数化设计	宇航材料工艺	2008，38（6）
24	鲍益东 陈文亮	讲　师 教　授	054	FAST SPRINGBACK SIMULATION OF BENDING FORMING BASED ON ONE-STEP INVERSE ANALYSIS	International Journal of Modern Physics B	2008, 22(31/32)
25	李迎光 潘志毅 闫瑞杰 廖文和	教　授 博士生 硕士生 教　授	054	A PDM-Based Framework for Collaborative Aircraft Tooling Design	International Journal of Production Research	2008, 46(9)
26	李迎光 方挺立 程少杰廖文和	教　授 博士生 硕士生 教　授	054	Research on feature-based rapid programming for aircraft NC parts	Applied Mechanics and Materials	2008, 10-12
27	李迎光 潘志毅 闫瑞杰 简建帮	教　授 博士生 硕士生 硕士生	054	An Aircraft Tooling Cooperative Design Model Based on Neuron-Endocrine-Immunity Working Principle	Journal of Advanced Materials Research	2008, 44-46
28	闫瑞杰 李迎光 潘志毅 廖文和	硕士生 教　授 博士生 教　授	054	A multi-agent-based semantic collaboration framework for aircraft tooling design and application	Proceedings of the 2008 12th International Conference on Computer Supported Cooperative Work in Design	Apr 16-18 2008
29	潘志毅 李迎光 黄　翔	博士生 教　授 教　授	054	A novel concurrent design process planning method and application	Proceedings of the 2008 12th International Conference on Computer Supported Cooperative Work in Design	Apr 16-18 2008
30	程少杰 李迎光	硕士生 教　授	054	基于痕迹法的槽腔特征识别方法	机械制造与自动化	2008，37（2）

31	闫瑞杰 李迎光 潘志毅	硕士生 教　授 博士生	054	基于TeamCenter Engineering的飞机工装语义协同设计技术研究	中国制造业信息化	2008，37（3）
32	易俊杰 刘长毅	硕士生 副教授	054	钛合金TC4超声波振动切削有限元仿真	中国制造业信息化	2008, 37(23)
33	刘长毅 于连友 田　威 唐金成	副教授 高　工 讲　师 高　工	054	Experiments of laser surface engineering for the green remanufacturing of railway coupler	Key Engineering Materials	2008，373-374
34	刘长毅 仇卫华 田威	副教授 硕士生 讲　师	054	铁路车辆车钩再制造激光表面熔覆温度场有限元分析	应用激光	2008，28(6)
35	刘长毅 张业勤 孙　莉	副教授 硕士生 硕士生	054	Web based 3D Assembly Sequence Planning Prototype Integrated with CAD Model	the 2008 12th International Conference on Computer Supported Cooperative Work in Design	
36	朱敏伟 周来水	硕士生 教　授	054	数控切割软件中TrueType字体的提取和处理	机械工程与自动化	2008, (5)
37	冯　鲜 周来水	硕士生 教　授	054	基于实体造型的三轴雕刻机仿真系统的 研究	机械工程与自动化	2008,　(5)
38	庄伟娜 周来水 安鲁陵 姬俊锋	硕士生 教　授 教　授 博士生	054	基于UG整体叶轮实体造型研究	中国制造业信息化	2008,37(5)
39	庄伟娜 周来水 安鲁陵	硕士生 教　授 教　授	054	基于UG的叶轮实体造型研究	CAD/CAM与制造业信息化	2008,　(9)
40	姬俊锋 周来水 安鲁陵 庄伟娜	博士生 教　授 教　授 硕士生	054	自由曲面叶片数控加工刀具轨迹规划方法	机械科学与技术	2008,27(5)
41	陈　功 周来水 安鲁陵 詹　雯	博士生 教　授 教　授 硕士生	054	基于网格边的复杂曲面优化展开	东南大学学报(自然科学版)	2008,38(2)
42	王　坚 周来水	博士生 教　授	054	基于最大权团的曲面粗匹配算法	计算机辅助设计与图形学学报	2008,20(2)
43	王玉国 周来水 安鲁陵 顾步云	博士生 教　授 教　授 博士生	054	型腔铣削加工光滑螺旋刀轨生成算法	航空学报	2008,29(1)
44	王玉国 周来水 安鲁陵 贾彤明	博士生 教　授 教　授 硕士生	054	二维轮廓嵌套加工刀轨生成算法	中国机械工程	2008,19(3)
45	李　涛 周来水 顾步云	博士生 教　授 博士生	054	基于几何约束的Doo-Sabin细分曲面修改算法	中国机械工程	2008,19(4)
46	李　涛 周来水 张唯中	博士生 教　授	054	C-C细分曲面的交互形状修改	中国图象图形学报	2008,13(1)

47	李　涛 周来水	博士生 教　授	054	基于平方距离极小化方法用C-C细分曲面拟合三角网	南京航空航天大学学报	2008，40(3)
48	李枫 陈明和 范平 王荣华 朱丽瑛 周兆峰	硕士生 教授 硕士生 硕士生 硕士生 硕士生	054	超塑成形扩散焊接组合工艺的技术概况与应用	新技术新工艺	2008，(4)
49	王荣华 陈明和 陈国亮 范平 李枫 周兆峰	硕士生 教授 硕士生 硕士生 硕士生 硕士生	054	TC4钛合金盒形件超塑成形工艺	热加工工艺	2008，37(11)
50	周兆峰 陈明和 范平 王杨根 王荣华 李枫	硕士生 教授 硕士生 硕士生 硕士生 硕士生	054	钛合金热应力矫形试验装置的研制	新技术新工艺	2008
51	范平 陈明和 周兆峰 王荣华 朱丽瑛 李枫	硕士生 教授 硕士生 硕士生 硕士生 硕士生	054	板料高频感应热应力成形技术试验研究	锻压技术	2008，33(4)
52	陈伟 陈明和 王辉	硕士生 教授 博士生	054	BTi6431S高温钛合金盒形件超塑性成型工艺	机械工程材料	2008，32(6)
53	张　臣 周来水 安鲁陵 周儒荣	讲　师 教　授 教　授 教　授	054	刀具变形引起的球头铣刀加工误差建模	南京航空航天大学学报	2008，40(1)
54	张　臣 周来水 安鲁陵 周儒荣	讲　师 教　授 教　授 教　授	054	球头铣刀刀具磨损建模与误差补偿	机械工程学报	2008，44(2)
55	王小平 安鲁陵 张丽艳 周来水	副教授 教　授 教　授 教　授	054	Uniform Coverage of Fibres over Open-contoured Freeform Structure Based on Arc-length Parameter	Chinese Journal of Aeronautics	2008，21(6)
56	徐　岩 李泷杲 高霖	副教授 讲　师 教　授	054	摩擦圆辊直径与摩擦包角对板成形摩擦系数测量的影响	机械科学与技术	2008，27，3
57	徐　岩 高霖 李泷杲	副教授 教　授 讲　师	054	基于管液压胀形的不锈钢焊管焊缝性能分析	中国机械工程	2008，19，9
58	徐　岩 L.C.Chan Y.C.Tsien	副教授 教　授 教　授	054	Prediction of work-hardening coefficient and exponential by adaptive inverse finite element method for tubular material	Journal of Materials Processing Technology	2008，201，3
59	毛俊东 徐　岩	研究生 副教授	054	润滑对板料胀形和拉伸性能的影响	机械制造与自动化	2008，37，5

60	闫崇京 廖和文 郭宇 程悠胜 高世文	博士生 讲师 教授 副教授 教授	054	Capability Based Manufacturing Service Rough Matching	2008 Pacific-Asia Workshop on Computational Intelligence and Industrial Application	
61	宋利康 庄海军 周儒荣	博士生 教　授 教　授	054	电子签章系统的研究与实现	机械科学与技术	2008，27(1)
62	田威 廖文和 刘长毅 于连友	讲　师 教　授 副教授	054	基于绿色再制造的火车车钩裂纹激光修复和表面强化	应用激光	2008，28(2)
63	周晚林 陈建鹏	副教授 硕士生	054	压电层合智能结构冲击损伤自诊断方法的研究	振动与冲击	20 08 年27卷6期
64	Wanlin ZHO Jianpeng CHEN	副教授 硕士生	054	Location Method of Loads on Piezoelectric Smart Wing Structures	ICIC Express Letters	20 08 年2 卷3期
65	周晚林 刘骄剑	副教授 硕士生	054	模线图形数字化处理方法的研究	应用基础与工程科学学报	2008，16（1）
66	张湘玉 刘浩 廖文和	博士生 副教授 教授	054	一种简单有效的曲线变形方法及在轴变形中的应用	机械科学与技术	2008，27（5）
67	李秀娟 廖文和 刘浩 何钢	博士生 教授 副教授	054	基于流曲线曲面的双三次非均匀B样条曲线G1混合	中国科学院研究生院学报	2008，25(4)
68	原恩桃 廖文和 刘浩	博士生 教授 副教授	054	面向数控粗加工的自适应细分	计算机集成制造系统	2008，14(11)
69	张　霖 赵东标 张建明 杨志甫	博士 教授	054	中间尺度零件微细铣削加工工艺	东南大学学报	2008，38(4)
70	张　霖 赵东标 张建明 杨志甫	博士 教授	054	微细端铣削工件表面粗糙度的研究	中国机械工程	2008，19(6)
71	程筱胜	教授	054	三角网格牙颌模型上的牙弓线半自动探测方法	机械科学与技术	2008，27(8)
72	程筱胜	教授	054	计算机辅助技术在上颌骨缺损修复中的研究与应用	生物医学工程学杂志	2008，25(4)
73	戴宁 周永耀 廖文和 俞青	副教授 高工 教授 副教授	054	口腔修复体模型曲面局部变形设计研究与实现	中国生物医学工程学报	2008，27（3）：378-382，388
74	戴宁 周永耀 廖文和 俞青 程筱胜	副教授 高工 教授 副教授 研究员	054	口腔预备体颈缘线裁剪算法	中国生物医学工程学报	2008，27（3）：353-359

75	戴宁 程筱胜 廖文和 俞青	副教授 研究员 教授 副教授	054	Deformation Design Technology of Dental Restoration Model	Proceeding of the First International Conference on BioMedical Engineering and Informatics	2008.5, Hainan:793-799
76	戴 宁 周永耀 袁天然 俞青 廖文和	副教授 高工 博士生 副教授 教授	054	口腔预备体颈缘线的快速提取	华南理工大学学报（自然科学版）	2008，36（5）：128-134
77	戴宁 钮叶新 俞青 廖文和	副教授 硕士生 副教授 教授	054	贴面的计算机辅助设计与制造	生物医学工程学杂志	2008，25(5):1029-1033
78	李娜 陈文亮 翟建军	硕士生 教授 教授	054	面向数控加工过程的可重配置虚拟加工方法	中国制造业信息化	2008，35(19)
79	彭威 陈文亮 曾建江	博士生 教授 副教授	054	A shape modification algorithm with curve constraints	The 2008 World Congress in Computer Science, Computer Engineering, and Applied Computing. (CGVR'08)	
80	郝小忠 程筱胜 耿习琴 何 磊	助工 高工 助工 工程师	054	基于UG的涡盘参数化建模技术研究与实现	中国制造业信息化	2008，7(37)

International Journal of Machine Tools & Manufacture 48 (2008) 1688–1692

Contents lists available at ScienceDirect

International Journal of Machine Tools & Manufacture

journal homepage: www.elsevier.com/locate/ijmactool

Short Communication

Electric hot incremental forming: A novel technique

Guoqiang Fan [a,*], L. Gao [a,1], G. Hussain [a,2], Zhaoli Wu [b,3]

[a] College of Mechanical and Electrical Engineering, Nanjing University of Aeronautics and Astronautics, Nanjing 210016, PR China
[b] Tai'an Science and Technology Information Institute, PR China

ARTICLE INFO

Article history:
Received 8 July 2008
Received in revised form
23 July 2008
Accepted 24 July 2008
Available online 3 August 2008

Keywords:
Incremental forming
Electric heating
Process parameters
Formability

ABSTRACT

In the current work, a new method is proposed for hot incremental forming. The method is based on simple tooling and is easy to employ. It makes use of electric current for heating hard-to-form sheet metals at the tool–sheet interface in order to fully utilize the formability of these materials. The potential effect of processing parameters, namely current, tool size, feed rate and step size, on the formability are investigated using AZ31 magnesium. In addition to this, the shape distortion of $TiAl_2Mn_{1.5}$ titanium workpiece after hot forming has also been addressed herein. Experimental results demonstrate that this technique is feasible and easy to control.

1. Introduction

Incremental forming (IF) is an innovative numerically controlled sheet metal-forming process [1,2]. This method can replace existing conventional forming methods in order to produce low-cost small batches. The process can be classified into two major types: (1) two-point IF and (2) single-point IF [3]. The latter type is economically more attractive than the former, as it does not make use of any solid die to shape the components.

In spite of spending a great deal of work [4–7], the process yet has not been employed for industrial applications. To deploy it in industry, many challenges are still there to be resolved. Duflou et al. [8] have shown that local heating can improve the process performance. They employed a laser source for dynamic local heating of aluminum sheet. The cost of the set-up (laser source and accessories) used is high. This will directly affect the final product cost. On the other hand, the promise of IF is to produce components at low cost. This necessitates more simple and economical method. In the current study, preliminary advancement carried out in this direction is presented. An electric heating system was developed and employed for local heating of sheet at the tool–sheet interface. The suitability of the device was examined by forming hard-to-form sheet metals, in contrast to Duflou et al. Two materials, namely AZ31 magnesium and $TiAl_2Mn_{1.5}$ titanium, having low formability at room temperature were successfully formed. The current values required for their successful forming were investigated. The surface quality and formability were also investigated at varying operating parameters. In addition, how to decrease distortion in forming was also discussed.

2. Principle and equipment for electric hot forming

Fig. 1(a) describes the principle of electric hot IF. A DC power source (transformer), cables, forming tool and sheet blank constitute a closed circuit. According to the Joule's law, when DC current flows from the tool to sheet, the high-current density generates heat. This raises the temperature in the localized zone at the tool–sheet interface, which in turn increases the ductility of the material at the contact zone. To prevent the current flow to machine tool, an insulation made of polyethylene is provided as shown in Fig. 1(a). Duflou et al. [8] used a 3-axis beam positioning system in order to properly position the laser spot on the deformation point, as shown in Fig. 1(b), which increases the complexity of the set-up. However, in the current method, the current flows from the tool to the sheet and thus there is no need to employ such a system. In this way, the present technique is simple and easy to control as compared to laser-assisted forming.

* Corresponding author. Tel.: +86 134 0193 6716.
E-mail addresses: fgqnh@hotmail.com (G. Fan), meelgao@nuaa.edu.cn (L. Gao), gh_ghumman@yahoo.com (G. Hussain), markzhaoli@163.com (Z. Wu).
[1] Tel.: +86 138 1586 8506.
[2] Tel.: +86 136 7516 1625.
[3] Tel.: +86 133 5538 6111.

0890-6955/$ - see front matter © 2008 Elsevier Ltd. All rights reserved.
doi:10.1016/j.ijmachtools.2008.07.010

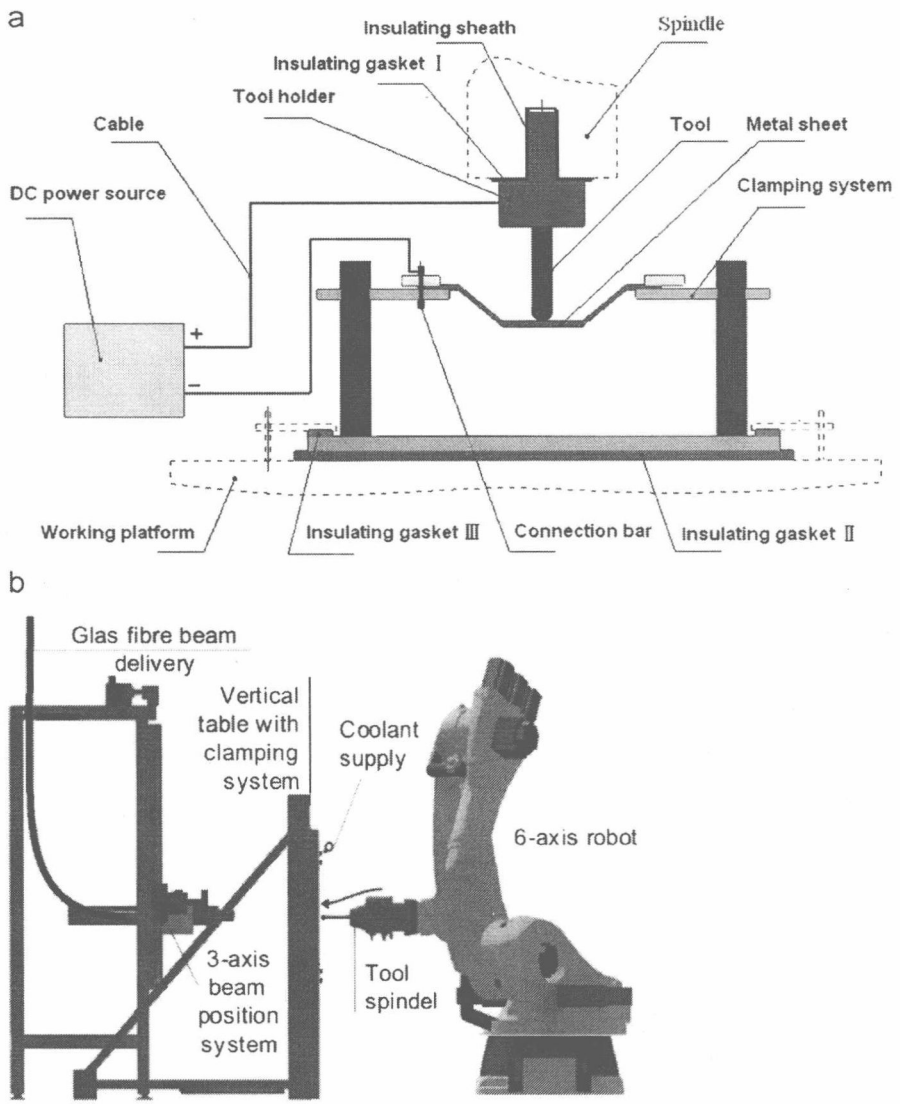

Fig. 1. (a) The principle of electric incremental forming and (b) the structure of the laser-assisted incremental forming machine.

3. Materials, tool and lubricant

In view of the low density and high specific strength, magnesium alloys are being considered for structural components in aerospace and automobile industries [9]. At the same time, titanium alloys with light mass and high specific strength are widely used in aeronautics and astronautics applications [10]. But magnesium and titanium alloys have low ductility at room temperature and offer much difficulty during forming. Therefore, these materials are normally formed at high temperatures. The current investigations were carried out with AZ31 magnesium and $TiAl_2Mn_{1.5}$ titanium alloys. The purpose of selecting these sheets was to check the adequacy of the newly introduced hot forming technique to provide enough temperature to successfully shape hard-to-form materials.

In hot forming, the selection of the tool material and the lubricant is very essential for successful forming. The tool was manufactured from tungsten carbide (YG8) and was brazed to the holder. In order to reduce friction at the tool/sheet interface, MoS_2 powder was dusted on the surface of the sheet metals as lubricant.

4. Investigations on the effect of optimal current on formability

4.1. Test description

In hot forming, the temperature directly affects the likelihood of part to be formed successfully. Since heating was carried out using electric current and this is rather complex to measure temperature at local point of heating, the current value was used as a criterion of successful forming. Due to limited availability of $TiAl_2Mn_{1.5}$ material, the experiments at varying current values were conducted with AZ31 of 1 mm thickness only. The formability was defined as the maximum wall angle (θmax) without sheet fracture. The wall angle corresponding to the fracture point was taken as θ_{max}, and it was determined by employing the varying wall angle conical frustum test, as defend in Hussain and Gao [11]. A conical frustum with continuously varying wall angle ranging from 30° to 90° was selected to evaluate the formability. Required object modeling and too-path programming were carried out in the commercial CAD/CAM software 'UG NX-3'. The forming tool traveled along the spiral tool path. The forming speed was set at 1000 mm/min, tool diameter was 8 mm and step size

Table 1
Formability test results of current

Current value (A)	Wall angle (°)	Remarks
300	44	No sheet burning
400	56	No sheet burning
500	64.3	No sheet burning
600	Failed	Sheet burns

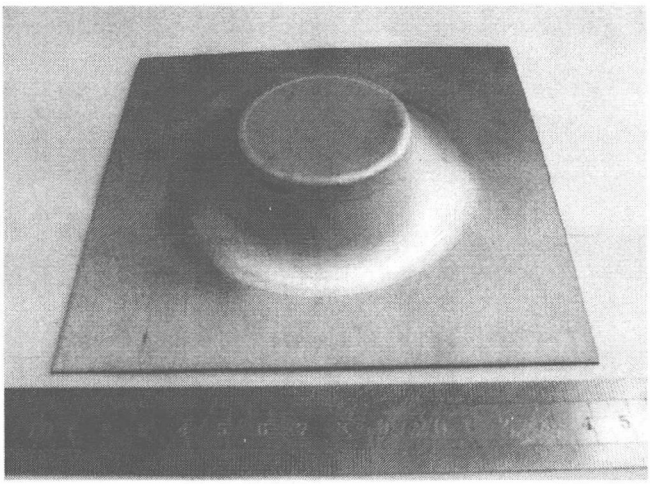

Fig. 2. AZ31 magnesium conical frustum.

was maintained at 0.2 mm for all the tests. The electric current value was varied from 300 to 600 A.

4.2. Results

Table 1 shows the surface quality and formability at different current values. As can be seen from the table, except for damaged workpieces, the wall angle is increased as the current value is increased. The maximum formability (64.3°) is achieved at the current value of 500 A (see Fig. 2). In fact, as the current value is increased, the temperature of the tool–workpiece contact zone is increased too. The yield strength of magnesium alloy sheet in the tool–workpiece contact zone is decreased, so the formability and the wall angle of magnesium alloy AZ31 is increased.

5. Investigation on the effect of processing parameters on formability

In the above section, current was found to be an important parameter for formability. However, if the other processing parameters, such as feed rate, tool diameter and step size, are altered, the current density will vary, which will affect the temperature at the tool/sheet interface. This means that the parameters other than current may also affect the formability. In this section, the influence of the aforementioned parameters will be simultaneously discussed. The current was kept constant at 500 A. The experiments were conducted with AZ31 of 1 mm thickness.

5.1. Feed rate

Table 2(a) presents the effect of feed rate on the formability. As can be seen from the table, too low or too high feed rate are unfavorable for formability. Except for the damaged workpiece achieved at the feed rate of 700 mm/min, the wall angle is decreased as the current value is increased. The maximum formability (64.3°) is achieved at the feed rate of 1000 mm/min. Too low feed rate causes sheet burning, while at too high feed rate, there is not enough time for the current to soften the sheet. In this way, both low and high feed rates are not acceptable. This means that, in electric hot forming, formability is dependent on feed rate.

Table 2
Formability test results of various processing parameters

(a) Formability test results of feed rate (tool diameter: 8 mm; step size: 0.2 mm; current: 500 A)

Feed rate	Wall angle	Remarks
700	Failed	Sheet burns
1000	64.3	No sheet burning
1300	53	No sheet burning
1600	43	No sheet burning

(b) Formability test results of tool diameter (feed rate: 1000 mm/min; step size: 0.2 mm; current: 500 A)

Tool diameter	Wall angle	Remarks
6	Failed	Sheet burns
8	64.3	No sheet burning
12	44.3	No sheet burning

(c) Formability test results of step size (feed rate: 1000 mm/min; tool diameter: 8 mm; current: 500 A)

Step size	Wall angle	Remarks
0.2	64.3	No sheet burning
0.3	49	No sheet burning
0.4	42	No sheet burning

5.2. Tool diameter

The effect of tool size on the formability and surface quality is shown in Table 2(b). This is to be seen from the table that, with the exclusion of the process failure, the wall angle is decreased as the tool diameter is increased. The process could not be executed when very small-sized tool (6 mm) was employed. Actually, very small-size tool concentrates the heat at extremely localized region and burns out the sheet. On the other hand, when the process is performed with large-sized tool, the heat is spread over relatively large zone of sheet, which cannot properly soften the sheet, leading to low formability. Therefore, the selection of proper tool size is very essential for successful electric forming.

5.3. Step size

Table 2(c) presents the influence of step size on the formability and surface quality. A trend can be seen from the table: smaller the step size, the larger the formability. It is obvious that, as the pitch is increased, the current density is decreased, and the heat generated by current is decreased too, so the formability of AZ31 magnesium is decreased.

6. Investigation on the effect of material resistivity on the temperature

According to the Joule's law ($Q = I^2Rt$), the quantity of heat generated by current is directly proportional to resistance. It is obvious that the resistivity of $TiAl_2Mn_{1.5}$ titanium is higher than that of AZ31 magnesium. As previously mentioned, when the tool

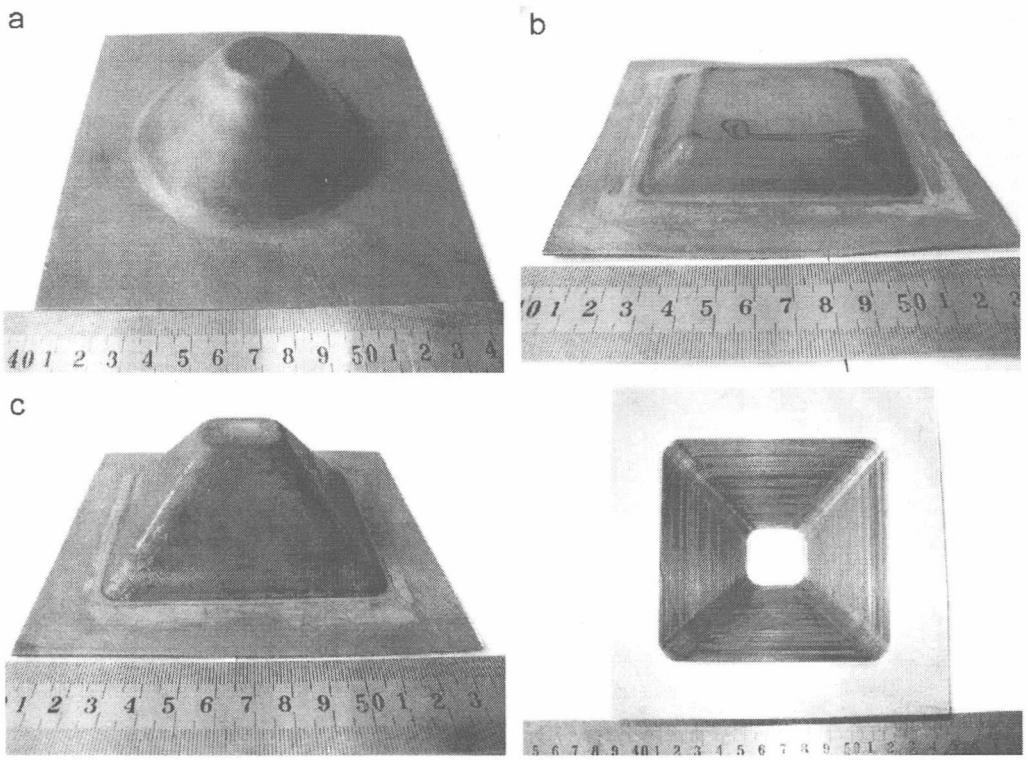

Fig. 3. $TiAl_2Mn_{1.5}$ workpieces: (a) a cone, current: 400 A; feed rate: 800 mm/min; step size: 0.1; tool diameter: 8 mm. (b) A distorted tetragonal pyramid, current: 400 A; feed rate: 800 mm/min; step size: 0.2; tool diameter: 12 mm. (c) A well-formed tetragonal pyramid, current: 400 A; feed rate: 400 mm/min; step size: 0.1; tool diameter: 8 mm.

diameter was 8 mm, pitch was 0.2 mm, feed rate was 1000 mm/min, and current was 500 A, the magnesium AZ31 sheet with 1 mm thickness could be well formed. That is to say, the temperature in the tool–workpiece contact zone did not reach 400 °C (the oxidation temperature of magnesium). The head of the tool and the magnesium sheet in the contact zone did not turn red. However, in same parameters, both $TiAl_2Mn_{1.5}$ sheet in the contact zone and the head of the tool turned red. The temperature is about 700 °C. This shows that sheet metals with high resistivity are relatively easy to acquire more heat.

7. Distortion of non-axial symmetry workpieces and solution

The residual stresses can affect the shape accuracy of the part after hot forming. In order to study this point, cones and pyramids with 50° were formed. The parts formed at various processing parameters are shown in Fig. 3. As can be seen from Fig. 3(a), cone has no distortion, while the pyramid is severely distorted (see Fig. 3(b)). This is due to the fact that the pyramid does not have a rotational symmetric shape and has stress gradient due to the presence of corners. While, cone is a rotational symmetric part and has relatively much smaller stress gradient as compared to the pyramid.

In order to decrease the local stress, the best way is to raise the temperature and reduce the feed rate to get sufficient forming. When small tool diameter (8 mm), small pitch (0.1 mm), and low feed rate (400 mm/min) in the beginning levels (up to 4 mm depth of pyramid) were adopted, a tetragonal pyramid was successfully formed without distortion (see Fig. 3(c)). At the same time, the surface was very smooth. Parameters adopted in formings are shown in Fig. 3.

8. Conclusions

In this study, a new hot forming method, for which a patent has been applied, is used to form hard-to-form sheet metals by the single-point IF process. The results obtained from the study using magnesium alloy and titanium alloy workpieces, lead to the following conclusions:

(1) The electric hot IF technique is feasible and easy to control. Probably the process could be used for other hard-to-form materials.
(2) Processing parameters, such as electric current, feed rate, tool diameter, step size, and resistivity, have effect on the formability of hard-to-form sheet metals. An increase in the electric current can increase the temperature and formability of hard-to-form sheet metals. On the contrary, an increase in feed rate, tool diameter, or step size can decrease the temperature and formability. In same parameters, the sheet metal with high resistivity can acquire more heat.
(3) After hot forming, asymmetric parts (such as pyramids) show more distortion than axisymmetric parts (such as cones). A strategy to eliminate distortion in electric hot forming was proposed.

References

[1] T. Maki, Sheet Fluid Forming and Sheet Dieless NC Forming, Amino Corporation, Japan.
[2] S. Matsubara, Incremental backward bulge forming of a sheet metal with a hemispherical head tool, Journal of JSTP 35 (1994) 1311.

[3] J.-J. Park, Y.-H. Kim, Fundamental studies on the incremental sheet metal forming technique, Journal of Materials Processing Technology 140 (2003) 447–453.
[4] H. Amino, Y. Lu, S. Ozawa, K. Fukuda, T. Maki, Dieless NC forming of automotive service panels, in: Proceedings of the Conference on Advanced Techniques of Plasticity, 2002, pp. 1015–1020.
[5] G. Ambrogio, L. De Napoli, L. Filice, F. Gagliardi, M. Muzzupappa, Application of incremental forming process for highly customized medical product manufacturing, Journal of Materials Processing Technology 162–163 (2005) 156–162.
[6] J.J. Park, Y. Kim, Fundamental studies on the incremental sheet metal forming technique, Journal of Materials Processing Technology 140 (2003) 447–453.
[7] J. Kopac, Z. Kampus, Incremental sheet metal forming on CNC milling machine-tool, Journal of Materials Processing Technology 162–163 (2005) 622–628.
[8] J.R. Duflou, B. Callebaut1, J. Verbert, H. De Baerdemaeker, Laser assisted incremental forming: formability and accuracy improvement, Annals of the CIRP 56/1/2007 273–276.
[9] K.U. Kainer, H. Dieringa, W. Dietzel, N. Hort, C. Blawert, in: M.O. Pekguleryuz, L.W.F. Mackenzie (Eds.), Metallurgy and Petroleum, Canadian Institute of Mining, Montreal, Canada, 2006, pp. 3–19.
[10] B.H. Hanson, M.W. Kearns, Properties and applications of titanium sheet [J], Sheet Metal Industries 59 (12) (1982) 877–878.
[11] G. Hussain, L. Gao, A novel method to test the thinning limits of sheet-metals in negative incremental forming, International Journal of Machine Tools and Manufacture 47 (2007) 419–435.

Available online at www.sciencedirect.com
ScienceDirect
ELSEVIER
International Journal of Machine Tools & Manufacture 48 (2008) 1170–1178
INTERNATIONAL JOURNAL OF MACHINE TOOLS & MANUFACTURE DESIGN, RESEARCH AND APPLICATION
www.elsevier.com/locate/ijmactool

Short Communication

An experimental study on the effect of thinning band on the sheet formability in negative incremental forming

G. Hussain*, N. Hayat, L. Gao

College of Mechanical and Electrical Engineering, Nanjing University of Aeronautics and Astronautics, 29-Yudao Street, Nanjing, Jiangsu 210016, PR China

Received 5 September 2007; received in revised form 21 January 2008; accepted 4 February 2008
Available online 20 February 2008

Abstract

In negative incremental forming, a characteristic thinning band occurs on the parts when wall angles approach the maximum obtainable [D. Young, J. Jeswiet, Wall thickness variations in single point incremental forming, Proceedings of the Institute of Mechanical Engineers, Part B, Journal of Engineering Manufacture 218 (2004) 1453–1459]. The effect of this ultra-thin band on the fracture occurrence of part was studied in the current investigation. It was found that the occurrence of a thinning band on the test specimen of a formability test does not mean an effect on the test result. A reduction in the formability due to the occurrence of the thinning band occurs only if the specimen fractures in the flange area. In order to evaluate the real forming limit of a sheet metal, a condition regarding the occurrence of part fracture is proposed.

Keywords: Negative incremental forming; Thinning band; Formability; Part fracture; Real forming limit

1. Introduction

Single-point incremental forming (SPIF) is a flexible sheet metal-forming process that is economically promising for low production-run manufacturing. In this process, a small-sized tool moves along a programmed tool path and shapes the part in an incremental fashion. The process is mainly performed by shear deformations, at least in the regions of the work piece where the horizontal radius of the curvature (ρ, as defined in Fig. 1(a)) is large [1]. The process has two principal variants: (1) positive incremental forming (PIF), and (2) negative incremental forming (NIF) [2].

It has been reported that, in NIF, a characteristic thinning band (see Fig. 1(b)) occurs along the surface of the part when wall angles (θ) approach the maximum achievable [3]. Also, the Sine law ($t = t_0 \cos\theta$, where t is the wall thickness, t_0 is the blank thickness and θ is the wall angle as defined in Fig. 1(b)) can not predict the part thickness in this unexpected band. As can be seen from Fig. 1(b), the part thickness in the band region is smaller than that of the remainder of the part. Therefore, if steeper walls are attempted, fracture will occur at this location prior to reaching the real forming limit of sheet. The effect of the thinning band on the sheet formability has not been investigated, in explicit terms. Moreover, no method to determine the actual forming limit of a sheet metal has been proposed in literature. The present work is an attempt in these directions. The experiments were performed with four different aluminum sheet metals. In order to quantify the formability, it was defined as the maximum wall angle (θ_{max}) without sheet fracture. The current study was carried out by employing the varying wall angle conical frustum (VWACF) test proposed by the authors in [4].

2. Part geometry and mathematical expressions

The part geometry employed for the present investigations is shown in Fig. 2(a). An arc of a circle with 115 mm radius (R) was used as a generatrix to generate the surface. This is obvious from the figure that the wall angle continuously increases along the generatrix from point $P_i(x_i, y_i)$ to $P_f(x_f, y_f)$, thus inducing a corresponding change

*Corresponding author. Tel.: +86 136 751 61625.
E-mail addresses: gh_ghumman@yahoo.com (G. Hussain), nasirhayat@uet.edu.pk (N. Hayat), meelgao@nuaa.edu.cn (L. Gao).

0890-6955/$ - see front matter © 2008 Elsevier Ltd. All rights reserved.
doi:10.1016/j.ijmachtools.2008.02.003

Nomenclature

σ_y	yield strength
σ_u	ultimate tensile strength
n	strain hardening index
K	strength co-efficient
δ	percent elongation in tensile test
θ	wall/forming angle of a part having constant slope (see Fig. 1(b))
θ_i	wall/forming angle at the initial point $P_i(x_i, y_i)$ of a part having varying wall angle (see Fig. 2(a)), or the wall angle imposed on the sheet in the beginning of the forming process
θ_f	wall/forming angle at the final point $P_f(x_f, y_f)$ of a part having varying wall angle (see Fig. 2(b))
θ_{max}	maximum wall angle that a sheet could endure without fracturing
$\theta_{i(critical)}$	the minimum value of θ_i on imposing which a thinning band affects the occurrence of part fracture, or the condition $h_d = h_b$ is met
R	radius of curvature of generatrix of part having varying wall angle (see Fig. 2(a))
ρ_i	curvature radius of the base of a part (see Fig. 2(a))
ρ_f	curvature radius of the bottom of a part (see Fig. 2(a))
h	design depth of part (see Fig. 2(a))
h_d	distance of fracture point, along y-axis, from the part flange (see Fig. 2(a))
h_b	distance of the extreme end of the thinning band from the part flange (see Fig. 3(b))
t_0	thickness of blank (see Fig. 1(a))
t/t_p	nominal wall thickness of part based on Sine law Eq. (2), or nominal wall thickness at an arbitrary point $P(x_p, y_p)$
$*t/*t_p$	actual wall thickness of part measured with a dial gauge, or actual wall thickness at an arbitrary point $P(x_p, y_p)$
$\varepsilon_{3(frac)}$	nominal fracture strain (in thickness direction) based on Eq. (3)
$*\varepsilon_{3(frac)}$	actual fracture strain (in thickness direction) based on actual thickness measured at fracture point
$\Delta\varepsilon$	deviation of actual fracture strain from the nominal one
S_{max}	maximum standard deviation
F_t	forming force imposed by the tool on the sheet prior to its fracturing

in the wall thickness (t) of the specimen (see [4] for details). Due to these variations in thickness, a fracture on a point $D(x_d, y_d)$ could occur whenever the thinning limit is surpassed. The instantaneous wall angle (θ_p) and the nominal thickness (t_p) on an arbitrary point $P(x_p, y_p)$ can be computed as derived in [4] and presented below

$$\theta_p = \cos^{-1}\left(\frac{y_p}{R}\right) = \cos^{-1}\left(\frac{y_i - h_p}{R}\right) \quad (1)$$

$$t_p = t_0 \cos\theta = \frac{t_0}{R}(y_i - h_p) \quad (2)$$

Making use of Eq. (2), the nominal thickness strain ($\varepsilon_{3(p)}$) on point $P(x_p, y_p)$can be calculated as

$$\varepsilon_{3(p)} = \ln\left(\frac{y_i - h_p}{R}\right) \quad (3)$$

To obtain its safe value, the wall angle at a point $M(x_m, y_m)$ situated 1 mm prior to the fracture point $D(x_d, y_d)$ (see Fig. 2(a)) was regarded as the maximum wall angle[1] θ_{max} without sheet fracture.

[1]During experiments it was observed that a part could be formed safely if the forming operation was terminated when the tool reached the depth (h_d-1) mm. Therefore, in case of fracture, the wall angle on the point corresponding to (h_d-1) can be regarded as the maximum wall angle without sheet fracture (see Fig. 2a).

3. Process parameters

The process of NIF is now well-known to the researcher's community. Its schematic representation along with the real experimental setup has been shown in a previous paper of the authors [4] and many others. For this reason, the process setup is not presented here. However, some important process parameters used in the experiments are as below:

Tool material = high-speed steel; radius of the hemispherical tool end = 4 mm; feed rate = 500 mm/min; step size = 0.32 mm/revolution; lubricant = machine oil; and blank size = 150 × 150 mm square.

4. Preliminary experiments and the design of test specimens

As mentioned previously, the thinning bands occur on the parts only when the wall angles approach the maximum attainable. Therefore, in order to design test specimens to investigate the effect of a thinning band on the formability of a sheet metal, an approximate value of the minimum initial wall/forming angle (θ_i), as defined in Fig. 2(a), on imposing which on a sheet a thinning band could occur was required. For this purpose, the VWACF tests were performed with four different sheet metals (see thickness and mechanical properties of sheets in Table 1) namely AA 2024 (annealed), AA 3003 (annealed), AA 1060-H24 (extremely strain-hardened) and AA 2024-T4 (tempered). The tests were conducted using the process parameters listed in Section 3, and the part dimensions as given in the

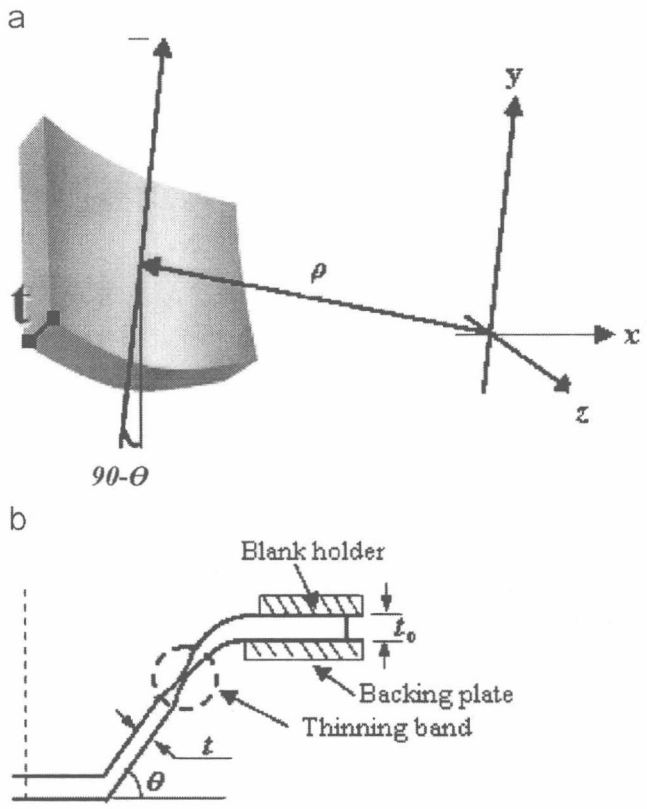

Fig. 1. (a) Definition of curvature radius ρ, and (b) schematic representation of a thinning band present on the part formed with constant wall angle θ.

footnote.[2] A set of parts of each sheet was formed by varying θ_i, in an equal increment of 4°, from 36° to 52°. In order to see the occurrence of a thinning band on a part, the wall thickness profile of each specimen was determined. To do so, a number of points (in an equal increment of 1 mm) were marked on the specimen's surface along the depth and the actual wall thickness ($*t$) was measured on each marked point. The points were marked with a depth gauge (0.01 mm least count), and $*t$ on a marked point was measured with a dial gauge (0.001 mm least count). The thickness profiles of the parts were examined and the deviation of the actual thickness from the nominal one (t based on Eq. (2)), was seen. It was found that three (AA 2024, AA 3003 and AA 2024-T4) of the four sheets showed thinning bands at about 52°, θ_i; there can be deviation of −3° in this value because θ_i was increased in the step of 4°. However, no thinning band occurred on the parts of the AA 2024-T4 sheet, as it could endure the maximum wall angle θ_{max} of only 47°. The value of θ_{max} (without any effect of the thinning band) for each sheet was also evaluated from these tests. An approximate value of θ_{max} obtained for four sheets is as follows: AA 2024: 69°, AA 3003: 81.5°, AA 1060-H24: 79° and AA 2024-T4: 47°. Since thinning bands did not occur on the parts of the AA 2024-T4 sheet, as stated earlier, it was dropped from the list of the potential materials needed for further experimentation. The formability of the AA 1060-H24 sheet was comparable to that of the AA 3003 sheet; therefore, further investigations were carried out only with two sheet metals, i.e., AA 2024 and AA 3003.

For further experimentation, a set of specimens, for each of the AA 2024 and AA 3003 sheets, with a variety of θ_i was designed (see Table 2). The value of θ_i was increased in small steps between 52° (or below as for the AA 2024 sheet) and the respective θ_{max} of each sheet, while the curvature radius (ρ_f) of the bottom underwent a variation due to variation in θ_i as clear from Fig. 2(b) and Table 2. The value of ρ_f in each specimen was kept large so as to avoid any negative effect of bi-axial stretching, which is dangerous for material formability as reported in [1], on the occurrence of sheet fracture.

5. Brief experimental procedure

The forming forces were measured by employing a force dynamometer (Kistler 9443B) under the forming fixture, as explained in [5]. The test specimens were formed to fracture using the process parameters listed earlier. Some representative test specimens formed for the current investigations are shown in Fig. 2(c).

The wall thickness profile of a specimen was outlined as described in the preceding section. The actual fracture strain ($*\varepsilon_{3(frac)}$) in thickness direction was computed, as reported in [6], using the following equation: and shown below: $*\varepsilon_{3(frac)} = \ln(*t_d/t_0)$, where $*t_d$ is the actual thickness measured on the fracture point $D(x_d, y_d)$ and t_0 is the blank thickness.

The nominal fracture strain ($\varepsilon_{3(frac)}$) on point $D(x_d, y_d)$ was calculated using Eq. (3). In order to determine the strain state at part fracture, the lengths (l_2) of the minor axes of the fractured grid circles, which (with 2 mm diameter (l)) were printed in ink on the sheet blanks before forming, were measured with a traveling microscope (0.01 mm least count). From a measured length l_2, the minor strain (ε_2) was calculated as: $\varepsilon_2 = \ln(l_2/l)$ and the corresponding major strain (ε_1) was computed using the relation: $\varepsilon_1 + \varepsilon_2 + \varepsilon_3 = 0$ (see [6] for details).

6. Results and discussion

Fig. 3(a) represents the fracture strain states of various parts made of two different sheets (AA 2024 and AA 3003). This is obvious from the figure that all the parts fractured in the same deformation mode, i.e., plane-strain stretching, as expected. Therefore, it can be said that the results of the formability tests to be discussed in the coming paragraphs are free of any negative effect of the hoop strains, i.e., ε_2.

[2]The curvature radius (ρ_i), as defined in Fig. 2(a), of the base of part was kept constant (55 mm) in each specimen of each sheet, and the final wall angle (θ_f) in each specimen of the AA 2024, AA 3003, AA 1086-H24 and AA 2024-T4 sheet was maintained at 75°, 85°, 85° and 60°, respectively.

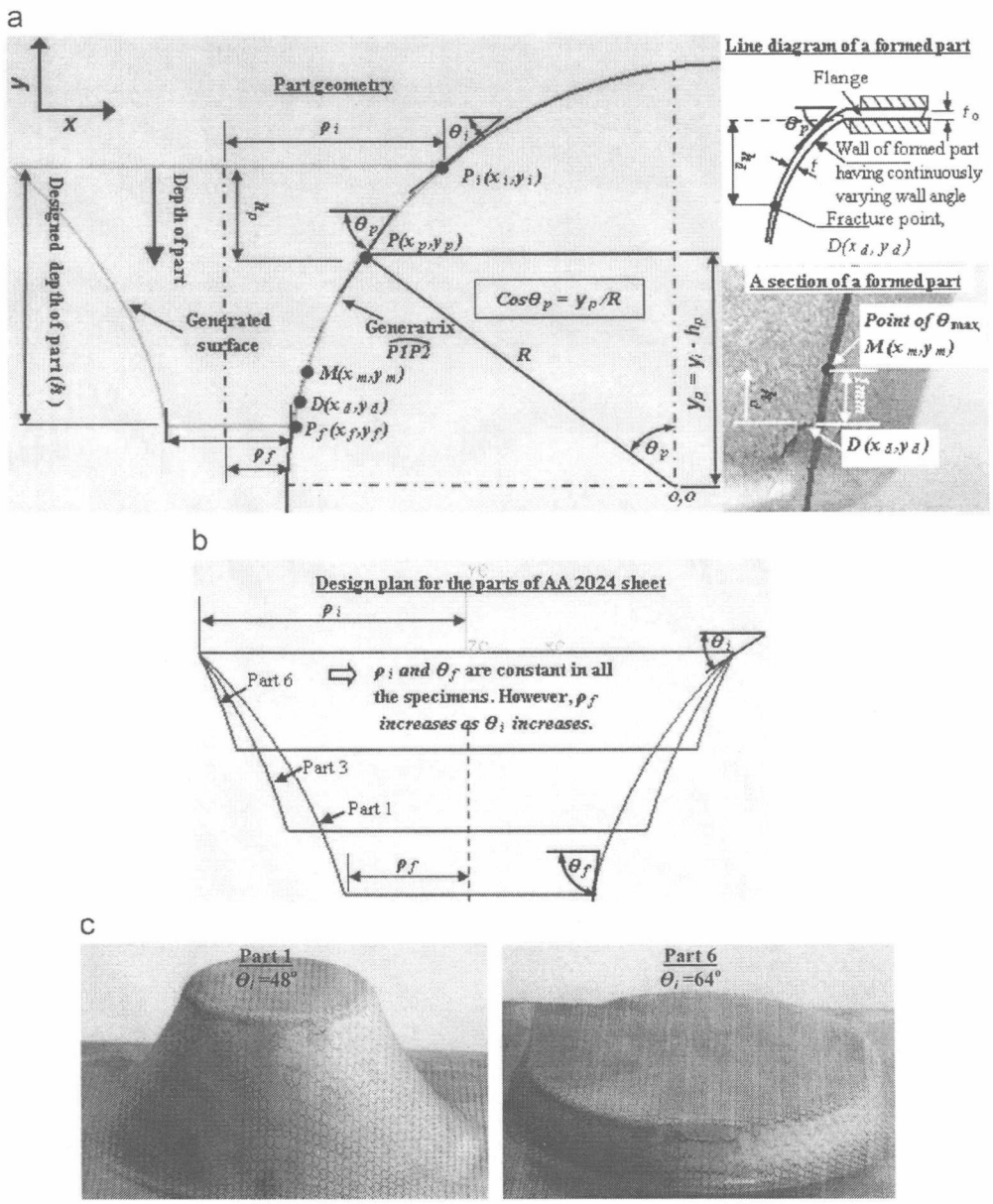

Fig. 2. (a) Part geometry, (b) methodology to design test specimens, and (c) some representative test specimens formed for the current investigations.

Table 1
Mechanical properties and the thickness of the experimental materials

Material type	σ_y (MPa)	σ_u (MPa)	n	K (MPa)	δ (%)	t_o (mm)
AA 2024	80.4	166.6	0.2	312	18.7	1.42
AA 3003	54.3	103.7	0.24	172	41	1.41
AA 1060-H24	132.6	140.4	0.08	171	5.5	1.2
AA 2024-T4	296.3	427.5	0.17	676	19.4	0.98

Note: See nomenclature for symbols.

Some examples of the thinning bands occurred on the parts of the AA 2024 sheet are presented in Fig. 3(b). The variations in the wall thickness of the parts indicate that two parts (parts 4 and 6) fractured due to the effect of the occurrence of the thinning bands and one part (part 2), inspite of having a thinning band, fractured normally (see deviation of wall thickness profile of each part from the nominal one). This is due to the fact that a thinning band occurs in the flange area of a part (see the wall thickness profiles and schematic shown in Fig. 3(b) and, therefore, affects the fracture occurrence of the part when the fracture limit of its base sheet metal falls in the flange area. In other words, the part fracture is affected by the thinning band when h_d becomes equal to h_b, where h_d is the distance of the fracture point from the part flange, and h_b is the distance of the extreme end of the thinning band from the part flange (see Fig. 3(b)). This can be seen from Fig. 3(c), that the minimum value of the initial forming